# SHEATH HYDRIDING MODEL FOR DEFECTIVE FUEL

G. Bruni, B.J. Lewis[A], W.T. Thompson[A]
Royal Military College, Ontario, Canada

## Abstract

A thermodynamic model for the Zr-H binary system at temperatures of 550°C and lower has been developed using the Gibbs energy minimization technique. This model is intended to provide terminal solubility concentrations of hydrogen in the $\alpha$-Zr phase in a fully mechanistic model for sheath hydriding of defective fuel now under development. The fundamental equations of the distribution of hydrogen in $\alpha$-Zr and ($\alpha$+$\delta$)-Zr, first introduced by Sawatzky, have been solved for and serve as a foundation for mechanistic model construction.

## 1. Introduction

Sheath hydriding results from a build up in hydrogen concentration in the fuel to sheath gap[B]. This highly unlikely phenomenon occurs as a result of coolant found in the gap which entered through a primary defect in the sheath while in reactor operation. This ingress coolant immediately flashes into steam and can contribute to hydrogen production through: (i) radiolytic decomposition of the steam, (ii) oxidation of the inner surface of sheath, (iii) $UO_2$ oxidation to $UO_{2+x}$ and/or (iv) dissolved hydrogen in the coolant [1]. Hydrogen production can lead to the formation of $ZrH_2$ within the sheath which has brittle properties that can lead to a secondary fuel element defect [2]. The schematic illustration of this process is shown in Figure 1.

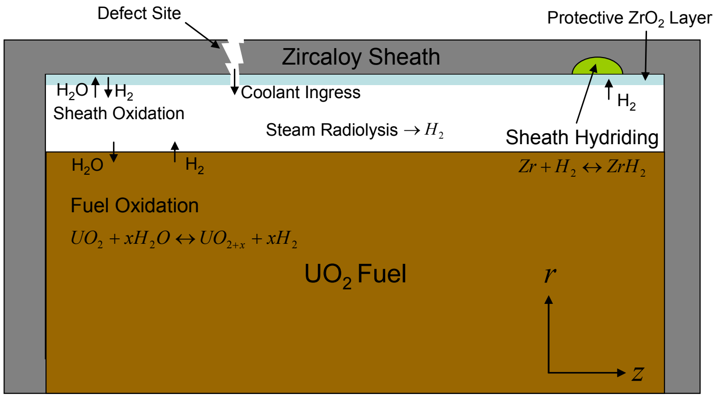

Figure 1: Schematic of the sheath hydriding process (modified from [1]).

The consumption of hydrogen caused by sheath hydriding effectively drives the fuel oxidation equilibrium, shown in Eq. (1), to the products side.

$$UO_2 + xH_2O \leftrightarrow UO_{2+x} + xH_2 \qquad (1)$$

---

[A] Thesis Supervisors
[B] In this paper reference will be made to $H_2O$ ingress and $H_2$ gas production but the discussion relates equally to $D_2O$ ingress and $D_2$ gas production as shown in [1].

Therefore, the consumption of hydrogen gas through sheath hydriding increases fuel oxidation. A mechanistic conceptual model for predicting fuel oxidation in defective fuel of water cooled reactors has been developed by Higgs [1] and accounts for fuel oxidation behaviour with dependence on sheath hydriding. No model for the hydriding behaviour was used; instead a 5% hydrogen pickup by the sheath was assumed. Therefore, there is a need for a fully mechanistic model for the hydriding of the sheath of defective fuel elements in water cooled reactors. The ultimate goal of this research is to provide a mechanistic model that links to the thermodynamics of the Zr-H Binary System analogous to the approach taken by Higgs in the fuel oxidation model [1] in linking that treatment to the U-O system thermodynamics.

## 2. Thermodynamic model of Zr-H binary system

Figure 2 shows the binary Zr-H phase diagram from the Bulletin of Alloy Phase Diagrams as well as a graph of partial pressure isotherms of $H_2$(g) in contact with zirconium at various H/Zr ratios. Both are based on the experimental data of [3].

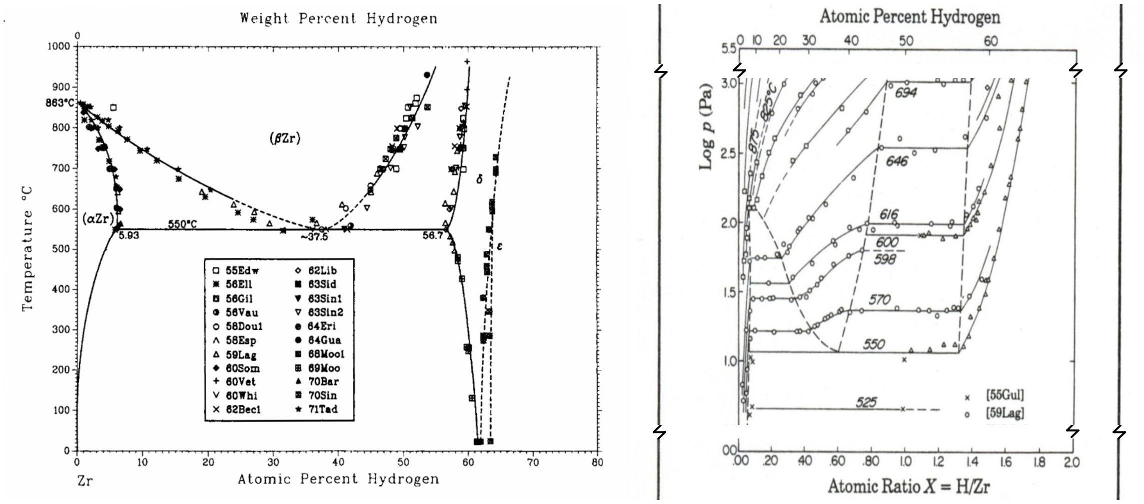

Figure 2: Zr-H binary phase diagram and graph of partial pressure isotherms of $H_2$(g) in contact with zirconium at various H/Zr ratios from experimental data of [3].

A thermodynamic model of the Zr-H system with consideration of the partial pressure of $H_2$(g) at temperatures at and below the eutectoid temperature (550ºC, well above water cooled reactor temperatures) was developed using Gibbs energy minimization techniques [4].

This model provides boundary conditions to a future mechanistic model of the hydriding of Zircaloy sheathing in water cooled type reactors and most importantly the at% of H required for saturation of the $\alpha$-Zr phase. This value is known as terminal solubility and marks the initiation of the hydriding reaction represented as

$$H_2(g) + Zr(\alpha) \rightarrow ZrH(\delta) \tag{2}$$

where the $\alpha$-Zr is the close packed hexagonal metallic phase and $\delta$-Zr is the hydride phase with a fluorite structure.

### 2.1 Phase component selection and corresponding composition scales

Since the thermodynamic model was limited to temperatures below 550ºC, only the $\alpha$ and $\delta$ zirconium phases were modelled. Each of these phases contains Zr and H as components which determine the composition and thermodynamic properties of their phase. However, modelling with these components for both the $\alpha$ and $\delta$ phases proved troublesome. For instance the $\alpha$ phase was modeled correctly on the zirconium rich side of the binary system but reappeared fictitiously at compositions higher than 65 at% H. It was concluded that both phases needed to be modelled with components that limited their composition ranges to those where they were thermodynamically stable.

This conclusion led to the use of a formal component, ZrH, in both the phases. The fact that this component may not be isolatable as a pure phase is secondary to it contributing to properly modelling the compositions and partial hydrogen gas pressures of the binary system. Table 1 outlines how each of the phases in the Zr-H binary system was modeled using the new ZrH component and their effective composition ranges. The $\beta$ phase is included in the table to show how it could be modelled in the future as a homogenous equilibrium.

Table 1: Component selection for the modeling of the Zr-H binary system

| Phase | Components | at% H Composition Range |
|---|---|---|
| $\alpha$ | Zr($\alpha$)[C] and ZrH($\alpha$) | 0-50 |
| $\delta$ | ZrH($\delta$) and $ZrH_2$($\delta$) | 50-66.67 |
| $\beta$ | Zr($\beta$) and ZrH($\beta$) and $ZrH_2$($\beta$) | 0-66.67 |

The conversion between the Zr and H component composition scale to the composition scale of the $\alpha$-Zr and $\delta$-Zr phases with their new components is important for analysis of the thermodynamic model.

The components of the $\alpha$ phase made up of Zr and H can be represented by the following equation:

$$aZr + bH \rightarrow cZr(\alpha) + dZrH(\alpha) \tag{3}$$

Performing a mass balance of the above equation gives two new equations that facilitate conversion between the two different composition scales.

$$\text{Given } X_H: \quad X_{ZrH}^{\alpha} = X_H / (1 - X_H) \quad \text{and} \quad X_{Zr}^{\alpha} = 1 - X_{ZrH}^{\alpha} \tag{4}$$

$$\text{Given } X_{ZrH}^{\alpha}: \quad X_H = X_{ZrH}^{\alpha} / (1 + X_{ZrH}^{\alpha}) \quad \text{and} \quad X_{Zr} = 1 - X_H \tag{5}$$

Figure 3 outlines various overall hydrogen compositions[D] in the $\alpha$ zirconium phase and the corresponding ZrH compositions.

---

[C] The $\alpha$ phase contains pure Zr metal allowing for Seivert's Law to hold (the dissociation of diatomic $H_2$(g) on the surface of α-Zr metal and atomic H being absorbed in metal).

[D] Note that "overall hydrogen composition" will be used to represent the composition of H in any phase as if the phase were modeled with the components Zr and H.

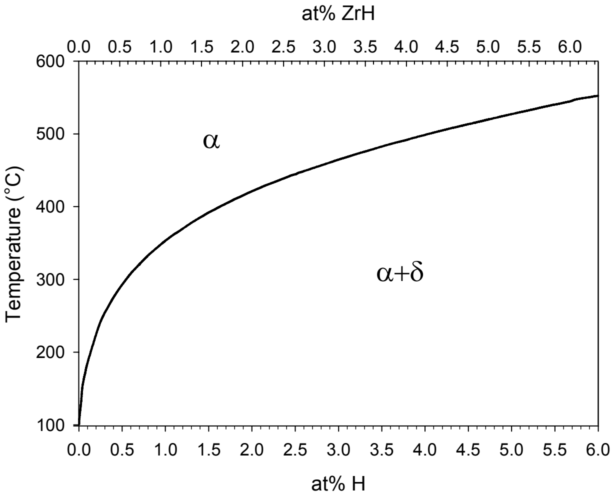

Figure 3: Plot of $\alpha$ /$\alpha$+$\delta$ phase boundary with both the atomic percent H and ZrH composition scales.

The $\delta$ phase has the narrowest composition range with the components of ZrH and $ZrH_2(\delta)$. The components can be represented from Zr and H by the following equation.

$$aZr + bH \rightarrow cZrH(\delta) + dZrH_2(\delta) \qquad (6)$$

Performing a mass balance of the above equation gives two equations that relate the two different composition scales for the $\delta$ phase.

$$\text{Given } X_H: \quad X^{\delta}_{ZrH_2} = (2X_H - 1)/(1 - X_H) \quad \text{and} \quad X^{\delta}_{ZrH} = 1 - X^{\delta}_{ZrH_2} \qquad (7)$$

$$\text{Given } X^{\delta}_{ZrH_2}: \quad X_H = (1 + X^{\delta}_{ZrH_2})/(2 + X^{\delta}_{ZrH_2}) \quad \text{and} \quad X_{Zr} = 1 - X_H \qquad (8)$$

Table 2 outlines various overall hydrogen compositions in the $\delta$ zirconium phase and the corresponding $ZrH_2(\delta)$ and $ZrH(\delta)$ compositions.

Table 2: Composition table $\delta$ for phase

| at% H | at% $ZrH_2(\delta)$ | at% $ZrH(\delta)$ |
|---|---|---|
| 50.00 | 0.00 | 100.00 |
| 52.00 | 8.33 | 91.67 |
| 54.00 | 17.39 | 82.61 |
| 56.00 | 27.27 | 72.73 |
| 58.00 | 38.10 | 61.90 |
| 60.00 | 50.00 | 50.00 |
| 62.00 | 63.16 | 36.84 |
| 64.00 | 77.78 | 22.22 |
| 66.00 | 94.12 | 5.88 |
| 66.67 | 100.00 | 0.00 |

## 2.2 Deriving thermodynamic properties of each phase

In order to model the $\alpha$ and $\delta$ phases using Gibbs energy minimization the thermodynamic properties of $ZrH(\alpha)$, $ZrH(\delta)$ and $ZrH_2(\delta)$ must be defined based on the components of each of these phases defined in Table 1. This will be done using a thermodynamic property known as the partial molar Gibbs energy.

In the Zr-H binary system, modelled for temperatures under the eutectoid temperature of 550ºC, there are 3 phases that need to be considered: $\alpha$-Zr, $\delta$-Zr and $H_2$ gas. How stable a given component is within a phase is defined by its partial molar Gibbs energy, $\overline{G_{componet}^{Phase}}$. This property shows how the total Gibbs energy of a phase $\mathbf{G}$ varies with an infinitely small change in the molar composition 'n' of the given component, so small that it the temperature, total pressure and composition of the mixture is not affected. The above description can be described by the following equation

$$\overline{G_{Component}^{Phase}} = \left( \frac{\partial \mathbf{G}^{Phase}}{\partial n_{component}} \right)_{T.P_T.composition} \tag{9}$$

A given component is most stable in a mixture where its partial molar Gibbs energy (also called chemical potential) is the lowest. For equilibrium to exist between two phases, any given component in the system must be equally thermodynamically favourable in either of the phases. With this condition, a small removal of any component from one phase (so small that it does not effect the overall composition of the phase) that is placed in the adjacent phase in equilibrium should require nor produce any Gibbs energy since both phases are equally stable.

For instance, when the $\alpha$ and $\delta$ phases of the Zr-H binary system are in equilibrium, three equations must be satisfied in order for this equilibrium condition to be true[E]

$$\overline{G_H^{\alpha}} = \overline{G_H^{G}} \tag{10}$$

$$\overline{G_H^{\alpha}} = \overline{G_H^{\delta}} \tag{11}$$

$$\overline{G_{Zr}^{\alpha}} = \overline{G_{Zr}^{\delta}} \tag{12}$$

The partial molar Gibbs energies of a the given component A in a phase, $\overline{G_A^{Phase}}$, can be represented as

$$\overline{G_A^{Phase}} = G_A^{0,REF} + RT \ln X_A + \overline{G_A^{Excess}} \tag{13}$$

where $G_A^{0,REF}$ is the Gibbs energy of A in its reference state, R is the universal gas constant, T is the temperature, $X_A$ is the mole fraction of A in the phase, and $\overline{G_A^{Excess}}$ is the excess Gibbs energy mixing term which in terms of $\alpha$ phase of the Zr-H system can be represented as $\overline{G_{Zr}^{Excess,\alpha}} = p_0^{\alpha} {X_{ZrH}^{\alpha}}^2$ and $\overline{G_{ZrH}^{Excess,\alpha}} = p_0^{\alpha} {X_{Zr}^{\alpha}}^2$ where $p_0^{\alpha}$ is the excess mixing parameter [4].

The partial molar Gibbs energy of H in the gaseous phase and Zr in the $\alpha$ phase can be easily defined using Eq. (13) as

---

[E] (i) Note that the partial molar Gibbs energy of Zr in the gaseous phase is not considered since it is assumed to be virtually involatile at temperatures below the eutectoid (550ºC). (ii) The gaseous phase is represented as atomic hydrogen gas H and is related to $H_2$ by the $0.5H_2(g) \leftrightarrow H(g)$ equilibrium.

$$\overline{G_H^G} = G_H^{0,G} + RT \ln P_H \tag{14}$$

$$\overline{G_{Zr}^\alpha} = G_{Zr}^{0,\alpha} + RT \ln X_{Zr}^\alpha + p_0^\alpha {X_{ZrH}^\alpha}^2 \tag{15}$$

$\overline{G_H^\alpha}$ , $\overline{G_H^\delta}$ and $\overline{G_{Zr}^\delta}$ are all based on the components H and Zr, which is not how the components of the $\alpha$ and $\delta$ phases are defined (Table 1). Therefore all three of these partial molar Gibbs energies must be rewritten. This is done by assuming that H or Zr is in a homogenous mixture with the defined components. The homogenous equilibria and the corresponding partial molar Gibbs energies, redefined, are shown in Table 3.

Table 3: Partial molar Gibbs energies redefined with phase components of Table 1.

| Homogenous equilibriums | Partial molar Gibbs energies redefined with phase components |
|---|---|
| $Zr(\alpha) + H(\alpha) \leftrightarrow ZrH(\alpha)$ | $\overline{G_H^\alpha} = \overline{G_{ZrH}^\alpha} - \overline{G_{Zr}^\alpha}$ |
| $ZrH(\delta) + H(\delta) \leftrightarrow ZrH_2(\delta)$ | $\overline{G_H^\delta} = \overline{G_{ZrH_2}^\delta} - \overline{G_{ZrH}^\delta}$ |
| $ZrH_2(\delta) + Zr(\delta) \leftrightarrow 2ZrH(\delta)$ | $\overline{G_{Zr}^\delta} = 2\overline{G_{ZrH}^\delta} - \overline{G_{ZrH_2}^\delta}$ |

The equations in Table 3 can be further developed with the following 3 equations.

$$\overline{G_{ZrH}^\alpha} = G_{ZrH}^{0,\alpha} + RT \ln X_{ZrH}^\alpha + p_0^\alpha {X_{Zr}^\alpha}^2 \tag{16}$$

$$\overline{G_{ZrH}^\delta} = G_{ZrH}^{0,\delta} + RT \ln X_{ZrH}^\delta + p_0^\delta {X_{ZrH_2}^\delta}^2 \tag{17}$$

$$\overline{G_{ZrH_2}^\delta} = G_{ZrH_2}^{0,\delta} + RT \ln X_{ZrH_2}^\delta + p_0^\delta {X_{ZrH}^\delta}^2 \tag{18}$$

Inserting Eq. (14) through (16) into Eq. (10) and assuming that there is ideal mixing of the formal components (i.e. $p_0^\alpha = 0$) the following equation results

$$\Delta G_{f,ZrH}^{0,\alpha} = RT \ln \frac{X_{Zr}^\alpha \cdot P_H}{X_{ZrH}^\alpha} + (G_H^{0,Gas} - 0.5 G_{H_2}^{0,Gas}) \tag{19}$$

where $\Delta G_{f,ZrH}^{0,\alpha}$ is defined as the Gibbs energy of formation of ZrH in the $\alpha$ phase expressed by the following equation.

$$Zr^\alpha + 0.5 H_2 \rightarrow ZrH^\alpha \tag{20}$$

The value of $\Delta G_{f,ZrH}^{0,\alpha}$ defines ZrH($\alpha$) for Gibbs energy minimization calculations of the Zr-H binary system. This value was found by solving Eq. (19) at 823K and 783K. $X_{Zr}^\alpha$ and $X_{ZrH}^\alpha$ were found using the hydrogen compositions in Figure 2 and $P_H$ was provided at 823K and 783K by experimental data in [3]. The value of $G_H^{0,Gas} - 0.5 G_{H_2}^{0,Gas}$ was easily determined using thermodynamic data from the F*A*C*T database at 823K and 783K [4]. Table 4 shows $\Delta G_{f,ZrH}^{0,\alpha}$ normalized to 298K and its corresponding enthalpy, entropy and specific heat capacity used to give the temperature dependence of $\Delta G_{f,ZrH}^{0,\alpha}$. The absolute entropy of ZrH(α) was calculated using

$$\Delta S^0_{f,298K} = -d\Delta G^0_{f,T} / dT = (S^0_{ZrH} - S^0_{Zr} - 0.5S^0_{H_2})_{298K} \tag{21}$$

The heat capacity of ZrH(α) was calculated assuming that $\Delta C_p$ of Eq. (20) is 0 and

$$C_p^{ZrH} = (C_p^{Zr^\alpha} + 0.5C_p^{H_2})_{800K} \tag{22}$$

Table 4: Thermodynamic values of formal component ZrH(*α*)

| $\Delta G^{0,\alpha}_{f,ZrH,298K}$ (J.mol$^{-1}$) | $\Delta H^{0,\alpha}_{f,ZrH,298K}$ (J.mol$^{-1}$) | $S^{0,\alpha}_{ZrH,298K}$ (J.K$^{-1}$.mol) | $C_p^{ZrH^\alpha}$ (J.K$^{-1}$.mol) |
|---|---|---|---|
| -70499 | -55220 | 51.27 | 43.79 |

The *α* phase is modelled as an ideal solution of Zr(*α*) and ZrH(*α*). Consider now the *δ* phase. Inserting Eq. (15) through (18) into Eq. (11) and assuming ideal mixing of components in each phase (i.e. $p_0^\alpha = 0$ and $p_0^\delta = 0$), the following equation results

$$\Delta G^{0,\delta}_{f,ZrH} - \Delta G^{0,\delta}_{f,ZrH_2} = -\Delta G^{0,\alpha}_{f,ZrH} + RT\ln\frac{X^\delta_{ZrH_2}\cdot X^\alpha_{Zr}}{X^\alpha_{ZrH}\cdot X^\delta_{ZrH}} \tag{23}$$

Inserting Eq. (15), (17) and (18) into Eq. (12), and again assuming ideal mixing of components in each phase (i.e. $p_0^\alpha = 0$ and $p_0^\delta = 0$), the following equation results

$$\Delta G^{0,\delta}_{f,ZrH_2} - 2\Delta G^{0,\delta}_{f,ZrH} = RT\ln\frac{{X^\delta_{ZrH}}^2}{X^\alpha_{Zr}\cdot X^\delta_{ZrH_2}} \tag{24}$$

Eq. (23) and (24) contain the unknown Gibbs energies of formation $\Delta G^{0,\delta}_{f,ZrH}$ and $\Delta G^{0,\delta}_{f,ZrH_2}$ which can be defined, respectively, as

$$Zr^\alpha + 0.5H_2 \rightarrow ZrH^\delta \tag{25}$$

$$Zr^\alpha + H_2 \rightarrow ZrH_2^\delta \tag{26}$$

These two Gibbs energies of formation are used in the Gibbs energy minimization calculations to model the *δ* phase in Zr-H system. The ZrH(*δ*) and ZrH$_2$(*δ*) mixing are taken to be ideal. Eq. (23) and (24) were solved using experimental composition data from [3] at the eutectoid temperature of 823K and it was found that $\Delta G^{0,\delta}_{f,ZrH_2}$ = -54595 J.mol$^{-1}$ and $\Delta G^{0,\delta}_{f,ZrH}$ = -29009 J.mol$^{-1}$.

The component of ZrH$_2$(*δ*) is well documented and experimental thermodynamic data is provided for this component in [3]. The literature data shows good agreement to the data in Table 5 which shows $\Delta G^{0,\delta}_{f,ZrH_2}$ normalized to 298K with its corresponding enthalpy of formation. The specific entropy and specific heat capacity values of ZrH$_2$ were used from [3].

Table 5: Thermodynamic data at 298K for $ZrH_2(\delta)$.

| $\Delta G^{0,\delta}_{f,ZrH_2}$ (kJ.mol$^{-1}$) | $\Delta H^{0,\delta}_{f,ZrH_2}$ (kJ.mol$^{-1}$) | $S^{0,\delta}_{ZrH_2}$ (J.K$^{-1}$.mol) | $C_p^{ZrH_2^\delta}$ (J.K$^{-1}$.mol) |
|---|---|---|---|
| -132.8 | -172.8 | 35.04 ± 0.08 | 30.95 ± 0.06 |

Since the thermodynamic data calculated for $ZrH_2(\delta)$ at 823K agrees well with the literature values provided in [3], the temperature dependence required for the $\alpha$+$\delta$/$\delta$ phase boundary was modelled with $\Delta G^{0,\delta}_{f,ZrH}$. This was done by first normalizing the $\Delta G^{0,\delta}_{f,ZrH}$ value at 823K to 298K. Then the specific entropy and heat capacity was initially set to the values found for ZrH($\alpha$) in Table 4 and using $\Delta G = \Delta H - T\Delta S$ the corresponding enthalpy was calculated. Finally the entropy was altered to match as well as possible the temperature dependence of the $\alpha$+$\delta$/$\delta$ phase boundary while correspondingly changing the enthalpy in order to maintain the value of $\Delta G^{0,\delta}_{f,ZrH}$ at 298K. The result for the specific entropy and enthalpy of formation at 298K best representing the temperature dependence of the $\alpha$/$\alpha$+$\delta$ phase boundary is shown in Table 6.

Table 6: Thermodynamic values for ZrH($\delta$) at 298K

| $\Delta G^{0,\delta}_{f,ZrH}$ (J.mol$^{-1}$) | $\Delta H^{0,\delta}_{f,ZrH}$ (J.mol$^{-1}$) | $S^{0,\delta}_{ZrH}$ (J.K$^{-1}$.mol) | $C_p^{ZrH^\delta}$ (J.K$^{-1}$.mol) |
|---|---|---|---|
| -65438 | -86642 | 33.00 | 43.79 |

## 2.3 Comparison of thermodynamic model to experimental data

Using the thermodynamic values for ZrH($\alpha$) in Table 4, $ZrH_2(\delta)$ in Table 5 and ZrH($\delta$) in Table 6 a complete model for the $\alpha$ and $\delta$ equilibrium was obtained using Gibbs energy minimization. Figure 4 shows this model in red superimposed onto the average of the experimental data from Figure 2.

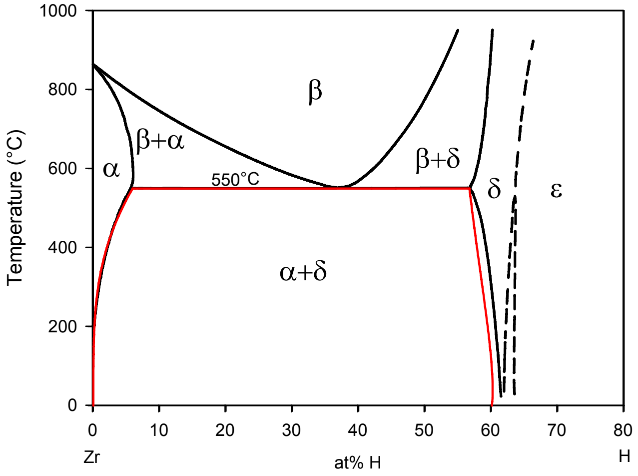

Figure 4: Thermodynamic model and experimental data comparison of $\alpha$/$\delta$ equilibrium.

Specific points along the $\alpha/\alpha+\delta$ phase boundary of the Zr-H binary system and the partial pressure of $H_2$(g) corresponding to these points provides critical data to the kinetics of the hydriding sheath process. Figure 5 shows a comparison of the experimental data of [3] to the thermodynamic model along this phase boundary including $H_2$(g) isotherms.

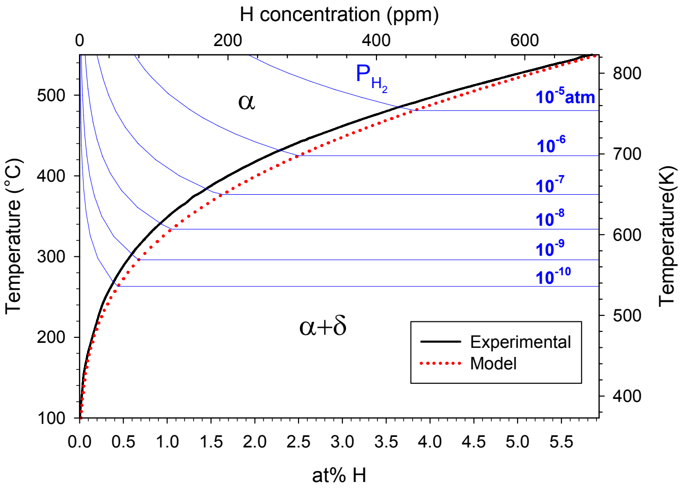

Figure 5: Model comparison of critical $\alpha/\alpha+\delta$ phase boundary with $H_2$(g) isotherms which bears comparison to Figure 2.

Figures 4 and 5 show that there is good agreement between the model and the experimental data provided in [3]. The above model is ideal with no mixing parameters introduced. This reinforces the need to select the right components when modelling phase equilibrium.

## 3. Steps to develop a model for massive hydriding

Initially hydrogen (in the fuel to sheath gap), in order to react with Zircaloy, must travel through a protective zirconium oxide layer on the inner surface of the sheath. This is done by slow volume diffusion where the diffusion rate is proportional to the thickness of the oxide layer [5]. Once the hydrogen reaches the surface of the sheath it dissolves in the $\alpha$-Zr phase. Hydrogen distributes in the radial and axial directions dependant on the distribution of concentration and temperature. The behaviour of this redistribution will be outlined further in the next section. Figure 6(i) outlines this first step of sheath hydriding.

A $\delta$- Zr hydride blister forms on the surface of the sheath when terminal solubility in the $\alpha$-Zr phase has been reached (Figure 6(ii)). The terminal solubility at a given temperature can be found using the critical points given in Figure 5 of the thermodynamic model proposed above.

Eventually a given hydride blister will grow to a critical thickness ($L_h$) and cause the protective oxide layer to crack (Figure 6(iii)). This is a result of the hydride having a 17% larger specific volume than $\alpha$-Zr [5]. This cracking allows direct hydrogen transport along the crack to the surface of the sheath resulting in more hydriding and more cracking of the oxide. This eventual fate is known as massive hydriding and can lead to a secondary defect in the sheath due to the brittle mechanical properties of the formed hydride (Figure 6(iv)). Secondary hydriding is the event generally associated with sheath deterioration and associated fission product release into the coolant.

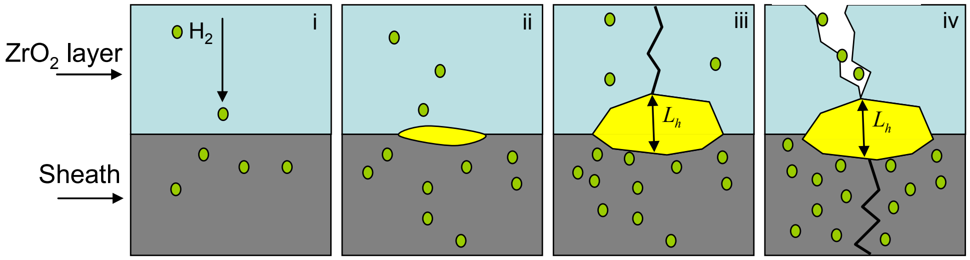

Figure 6: Steps to massive hydriding and secondary failure of sheath in water cooled reactors.

### 3.1 Hydrogen distribution in sheath

Hydrogen distribution or flux in the Zircaloy sheath is a result of two gradients: concentration and temperature. For instance the flux of hydrogen in $\alpha$ -Zr is represented by Eq. (27)

$$J_\alpha(r) = -D_\alpha(T)\left(\nabla N(r) + \frac{Q_\alpha^* N(r)}{RT^2}\nabla T(r)\right) \tag{27}$$

where N is the concentration of hydrogen in the $\alpha$-Zr solid solution, T the temperature and R the universal gas constant [7].

Fick's law defines the effect of a concentration gradient on the mass flux [6]. Hydrogen will migrate to areas of lower concentration. This value is temperature dependant as defined in Eq. (28)

$$D_\alpha(T) = D_\alpha^0 e^{\left(-\frac{Q_\alpha}{RT}\right)} \tag{28}$$

where $Q_\alpha$ is the activation energy for diffusion of hydrogen in the $\alpha$ phase [7].

The effect of a temperature gradient on the flux of hydrogen through zirconium is known as the Soret effect or thermal diffusion. The direction of mass flux due to thermal diffusion is defined by the heat of transport $Q_\alpha^*$ for the given mass [6]. The value for the heat of transport for hydrogen is positive and therefore hydrogen migrates to the colder areas of the sheath due to a temperature gradient.

The concentration and thermal gradient force hydrogen to migrate to the colder and less hydrogen concentrated areas within the sheath. Using Eq. (27) and the continuity equation, $dC/dt = -dJ_\alpha/dr$, the H concentration in $\alpha$-Zr has been modelled in the 1-D radial direction by finite element analysis. Solving parameters were provided by Sawatzky [7] including a constant temperature gradient in the sheath $K = dT/dr$ and a temperature distribution in the sheath from $T_{cold} = 573K$ and $T_{hot} = 773K$.

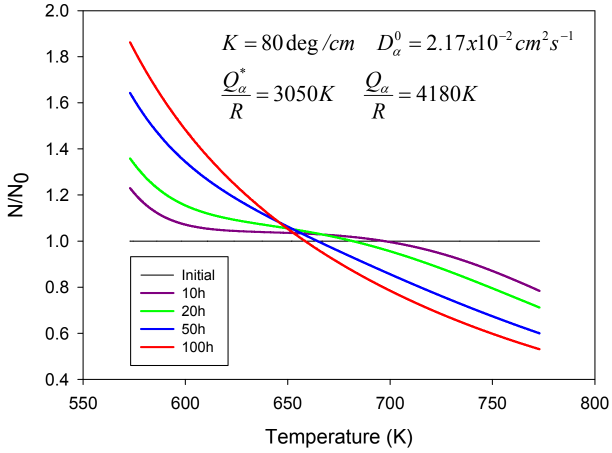

Figure 7: Numerical solution to Eq. (27) (T = 573K to 773K) using parameters given above.

The two phase region of ($\alpha$+$\delta$)-Zr can be described by Sawatzky's approximate model which assumes that diffusion of hydrogen in the $\delta$ phase is negligible and that the concentration of the $\alpha$ phase in the two phase region is its terminal solubility $N_\alpha$. Therefore the following equation applies

$$J_{\alpha+\delta}(r) = -D_\alpha(T)\left(\nabla N_\alpha(T) + \frac{Q_\alpha^* N_\alpha}{RT^2}\nabla T(r)\right) \qquad (29)$$

where $N_\alpha(T) = N_\alpha^0 e^{\left(\frac{-\Delta H}{RT}\right)}$ and $\Delta H$ is the heat of mixing.[7]

The concentration of hydrogen in the two phase region was solved analytically using the continuity equation and Eq. (29) with the solving parameters shown below. This solution along with the solution provided in Figure 7 can be used to model an overall hydrogen distribution in the sheath. From the work of Sawatzky it is known that the approximation of Eq. (29) is reasonable and that for large times the two phase region ($\alpha$+$\delta$) is present along with the one phase regions of $\alpha$ and $\delta$ [3].

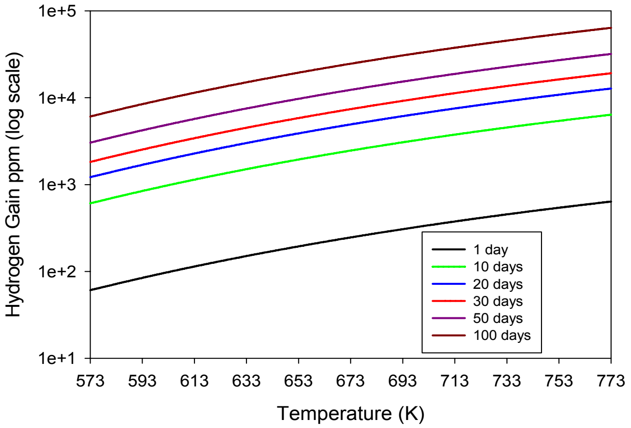

$$K = 100\deg/cm \quad D_\alpha^0 = 2.17x10^{-2}cm^2s^{-1}$$

$$\frac{Q_\alpha^*}{R} = 3015K \quad \frac{Q_\alpha}{R} = 4170K$$

$$N_\alpha^0 = 8.5x10^4\,ppm \quad \frac{\Delta H}{R} = 3820K.$$

Figure 8: Sawatzky's approximate model solved analytically

## 4. Conclusion

A reasonable thermodynamic model for the Zr-H binary system that involves the partial pressure of $H_2(g)$ has been developed. This could be further improved by the introduction of small excess Gibbs energy mixing terms formulated from the data of planned experimentation. This is to be linked to a mechanistic model describing the kinetics of the hydriding of sheath in a defective element. The fundamental distribution equations, introduced by Sawatzky, for hydrogen in the single phase $\alpha$ and two phase $\alpha+\delta$ region have been solved for and can be used in a future model to describe the entire distribution of hydrogen in the sheath. With a better understanding of sheath hydriding in a more detailed and quantitative way, it may be possible to fundamentally predict the onset of secondary hydriding. As such, one could discharge the bundle from the reactor in its normal operating cycle before significant fission product release would occur.

## 5. Acknowledgements

CANDU Owners Group (COG), University Network of Excellence in Nuclear Engineering (UNENE) and National Sciences and Engineering Research Council (NSERC) for financial support of this research.

## 6. References

[1] J.D. Higgs, B.J. Lewis, W.T. Thompson and Z. He, “A conceptual model for the fuel oxidation of defective fuel”, *Journal of Nuclear Materials*, 366 (2007), 99-128.

[2] Yeon soo Kim, Wei-E Wang, D.R. Olander and Suresh K. Yagnik, “High-pressure hydriding of Zircaloy”, *Journal of Nuclear Materials*, 240 (1996), 27-31.

[3] E.Zuzek, J.P. Abriata, A. San Martin and F.D. Manchester, “The H-Zr (Hydrogen-Zirconium) System”, *Bulletin of Alloy Phase Diagrams*. Vol.11 No. 4 (1990) 386.

[4] C.W. Bale, A.D. Pelton, and W.T. Thompson. “**F**acility for the **A**nalysis of **C**hemical **T**hermodynamics” Ninth International Conference on High Temperature Materials Chemistry: May 19-23, Penn State, Pennsylvania.

[5] E.Yu Afanas’eva, I.A. Evdokimov, V.V. Likhanskii, A.A. Sorokin, O.V. Khorizhii and V.V. Nivikov. Likhanski, “Simulation of the hydriding failure of fuel elements in water-cooled reactors”, *Atomic Energy*, 95, no. 4(2003), 689-695.

[6] D.R. Olander, Fundamental Aspects of Nuclear Reactor Fuel Elements, National Technical Information Service, University of California, Berkley, 1976, 70-79.

[7] Anton Sawatzky and Erich Vogt, “Mathematics of Thermal Diffusion of Hydrogen in Zircaloy-2”, Atomic Energy of Canada, AECL-1411, Chalk River, Ontario, October 1971.